Study on the Effect of Electrical Conductivity on Road Surface Wetness Classification Using Capacitive Measurement Data

Jakob Döring, Lukas Lütkehaus, and Karl-Ludwig Krieger

***Abstract*—As the friction between a vehicle's tires and the road surface correlates with the road-covering water film height, knowledge about the present wetness level is of relevance for drivers and autonomous systems. A promising approach for wetness quantification is based on a capacitive transducer array (TA) that is integrated at a front wheel arch liner and capable of detecting spray water ejected by the tires. While this approach has already shown that wetness classification using capacitive measurement data is feasible, potentially affecting factors such as the water's electrical conductivity were assumed to be constant in the past. This article presents a study on the effect of the spray water's conductivity on wetness classification for that approach and also demonstrates the feasibility of classifying conductivity using the same capacitive measurement data. For these purposes, we propose a test bench capable of simulating reproducible spray water scenarios. We show the effect of varying conductivity on the measured capacitance curves complicating the distinction of wetness classes. In partial investigations, we demonstrate the extent of the conductivity's effect on classifier performance. While wetness classification with conductivities differing from training results in poor classifier performance, the mean accuracy (ACC) can be increased to approximately 0.98 considering all occurring conductivities. Furthermore, we propose a two-stage classification approach that initially determines the conductivity and subsequently considers it as an additional feature in wetness classification. The approach increases classifier performance to more than 0.99 indicating that knowledge of the spray's present conductivity can optimize road surface wetness classification.**

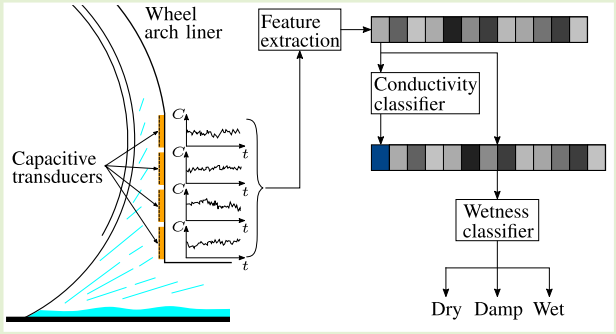

***Index Terms*—Capacitive sensors, electrical conductivity, machine learning, road surface wetness detection, vehicle safety, wetness classification.**

I. Introduction

DUE to lower friction between the road surface and a vehicle's tires, accident risk significantly increases on wet road surfaces [1], [2], [3]. The extent of friction reduction is dependent on the road-covering water film height which may vary from a few microns to several millimeters [4], [5]. Thus, knowledge about the current wetness level is of relevance for drivers and autonomous systems.

In [6], a promising approach for road surface wetness quantification was presented. It is based on a 2 × 4-planar capacitive transducer array (TA) integrated on a front wheel arch liner's rear-facing side and capable of detecting spray water ejected by the tires. An experimental study on a test track demonstrated the reliable assessment of wetness-related dependencies using the proposed capacitive sensor system. Moreover, a classifier was presented that is able to automatically distinguish between eight wetness levels with considerable performance. However, potentially affecting environmental factors like the typically unknown water's electrical conductivity were considered to be constant in the study.

As known from the literature, unless a medium's electrical conductivity is not negligibly small, it contributes to the complex permittivity and thus affects the absolute capacitance [7], [8]. In the context of water as a medium, various publications have presented experimental studies on the conductivity's effect on a capacitance measurement [9], [10]. While the effect is undesirable in the field of level monitoring, for example, it is exploited for water quality monitoring in order to draw conclusions about the water composition [11], [12].

Manuscript received 12 August 2022; accepted 25 August 2022. Date of publication 12 September 2022; date of current version 14 October 2022. This work was supported by the German Federal Ministry for Economic Affairs and Energy (BMWi) under Grant 19A16016D. The associate editor coordinating the review of this article and approving it for publication was Dr. Ravibabu Mulaveesala. *(Corresponding author: Jakob Döring.)*

The authors are with the Institute of Electrodynamics and Microelectronics, University of Bremen, 28359 Bremen, Germany (e-mail: doering@item.uni-bremen.de; l.luetkehaus@uni-bremen.de; krieger@item.uni-bremen.de).

Digital Object Identifier 10.1109/JSEN.2022.3204111

While the water's conductivity on the test track was assumed to be approximately constant in [6], significant deviations can occur under realistic conditions, as shown by various publications. Already the conductivity of rainwater can be subject to significant variations. In [13], conductivity median values in the range of 1 μS/cm $\leq \sigma \leq$ 26 μS/cm were found for harvested rainwater from air as well as roof coverings, and in [14], values in the range of 6 μS/cm $\leq \sigma \leq$ 33 μS/cm for rainwater collected from open ground were reported. In addition, vehicular and road contaminants can be expected to increase the water's conductivity, due to additional free charge carriers in the form of ions [15]. Studies on forest roads showed fluctuations in the range of approximately 50 μS/cm $\leq \sigma \leq$ 200 μS/cm [16]. In the extreme scenario, for contamination with road salt, conductivity of several mS/cm is realistic [17].

In this article, we study the effect of the spray water's electrical conductivity on road surface wetness classification. For this purpose, we simulate reproducible spray water scenarios with ten different conductivities under defined laboratory conditions on a test bench that includes a front wheel arch liner along with a 2 $\times$ 4-planar capacitive TA. We demonstrate the conductivity's effect on the capacitance signal for an exemplary scenario representing a specific wheel speed and a road surface wetness class. For acquired measurement data, we present an investigation regarding the effect on classifier performance. Moreover, we show that classification of the spray water's conductivity using capacitive measurement data is feasible. Furthermore, we propose a two-stage classification approach to optimize the class prediction for occurring conductivity differences.

The remainder of this article is organized as follows. In Section II, we present the experimental setup for data acquisition and illustrate the conductivity's effect on the measured capacitance characteristics. Section III outlines the results for classifying wetness levels in the presence of varying electrical conductivity. We discuss the results with respect to the conductivity's effect on classifier performance as well as for the proposed two-stage classification approach. Finally, a conclusion is drawn in Section IV.

II. Experiments

In this section, we describe the experimental setup around the sensor system used and the test bench developed. In addition, we outline the simulated spray scenarios and experiments for data acquisition. Here, we illustrate the general capacitance characteristics of a transducer (TD) as well as the effect of varying conductivity on these characteristics.

A. Sensor System

In this article, data acquisition is realized using a sensor system comprising a TA and application-specific sensor electronics. The individual components are described below.

1) TD Array: For the data acquisition in this article, a 2 $\times$ 4-planar capacitive TA is applied on a front wheel arch liner's rear-facing side. The individual TDs are manufactured as flexible printed circuit boards (PCBs) of size 54 $\times$ 54 $\times$ 0.2 mm^3. Due to their low thickness, they can be applied almost planarly

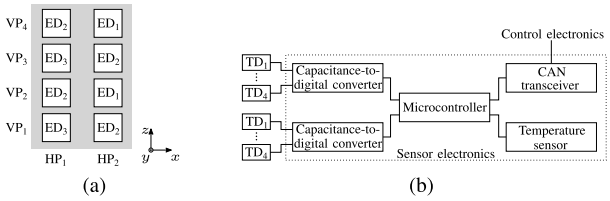

Fig. 1. Schematic representation of the (a) TA and the (b) sensor system.

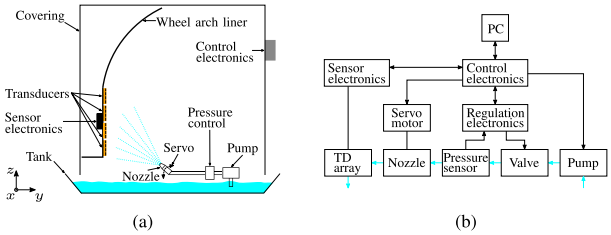

Fig. 2. (a) Schematic representation and (b) information flow of the test bench for simulating road wetness under laboratory conditions.

without significantly affecting the impinging and draining droplets' characteristics. Fig. 1(a) shows the arrangement of the eight TDs as a front view divided into horizontal (HPs) and vertical positions (VPs). In the following, the exact position is given by P_{xz}, where x corresponds to the HP and z to the VP. The detailed layering of the TDs, as well as the parameterization of the individual complementary electrode designs (EDs), corresponds to the description given in [18]. In brief, ED_1 provides the highest dynamic range and sensitivity for low amounts of water, whereas ED_2 is supposed to allow detection of larger quantities. ED_3, on the other hand, has the highest penetration depth and is designed to distinguish between very large water quantities. For more details on the EDs, which are out of the scope of the article, refer to [18].

2) Sensor Electronics: For reliable acquisition of the capacitive measurement data, application-specific sensor electronics are used, mounted in a waterproof housing behind the wheel arch liner. Fig. 1(b) shows the sensor electronics' block diagram. FDC2214 [19] represents the core component for recording and digitizing the capacitances. For this purpose, the capacitance-to-digital converter (CDC) uses LC resonators that are tuned to 100 kHz for data acquisition. In addition, the sensor electronics include a 32 bit microcontroller, a temperature sensor, and a controller area network (CAN) transceiver. The measurement data of the individual TDs are transmitted as int16 data type via CAN bus, resulting in a theoretical value range of -3276.8–3276.7 pF with a resolution of 0.1 pF and a sampling rate of 145 Hz.

B. Test Bench

In order to simulate different spray water scenarios, a test bench is implemented based on the fundamentals of water ejection by a tire and video recordings of test drives on wet road surfaces. Fig. 2(a) shows a schematic representation of the developed test bench for simulating road surface wetness. A key component is a front wheel arch liner including the TA and associated sensor electronics. Analogous to the positioning in a vehicle, it is mounted and aligned on a scaffold of aluminum profiles (for the sake of clarity, the illustration

TABLE I
VOLUMETRIC FLOW RATES OF THE FOUR USED FCNS ACCORDING TO THEIR DATA SHEETS

Nozzle	Volumetric flow rate [l/min]	
	1 bar	3 bar
FCN_a [22]	0.15	0.24
FCN_b [23]	0.27	0.47
FCN_c [23]	0.89	1.54
FCN_d [24]	2.28	4.00

of the scaffold is omitted). A membrane pump, which can generate a maximum pressure of 6.9 bar, transports water via a proportional valve and a pressure sensor through a tube to a full cone nozzle (FCN). The water is sprayed from this nozzle and impinges on the wheel arch liner as drops. The nozzle is vertically adjusted by a servomotor. Furthermore, a covering to prevent spray water from emerging enables a continuously filled water reservoir in the form of a collection tank, thus creating a closed water circuit.

The individual components' connections and the resulting information flow at the test bench are shown in Fig. 2(b). In addition to the sensor electronics, control electronics and regulation electronics are developed. The latter is used to regulate the pressure at the nozzle. The key component here is a microcontroller, which handles the digital control of the proportional valve as a proportional–integral–derivative (PID) controller. It receives the command variable from control electronics via interintegrated circuit (I^2C). A pressure sensor with a measuring range of 0–10 bar supplies the control variable. The calculated manipulated variable is transmitted to the input of the proportional valve via pulsewidth modulation (PWM). In addition to the target pressure, the control electronics also transmit the desired angle setting to the servomotor via PWM. Furthermore, the pump is switched by a metal–oxide–semiconductor field-effect transistor (MOSFET), and the sensor electronics' measurement data are received as well as processed via CAN. The control electronics transmit the capacitive measurement data, the sampling time, and the measured pressure to a personal computer (PC) using a serial interface.

C. Realized Scenarios

The circumferential spray to be simulated, which is the dominant spray type for the wheel arch liners, correlates with road surface wetness, wheel speed, and spray-off angle [6], [20]. While higher wheel speed leads to larger spray amounts and smaller drops due to a higher ejection frequency, greater road surface wetness results in larger amounts and bigger drops [21]. In addition, drop size and quantity decrease as the spray-off angle increases due to released water along the rotation.

The correlation to road wetness is realized using various FCNs that allow different volumetric flow rates and thus varying drop sizes and quantities at a defined pressure. Table I summarizes the flow rates of the four nozzles applied exemplarily for 1 and 3 bar. The amount of water increases with the applied pressure, analogous to an increase in wheel speed in the real use case. Furthermore, due to the FCNs' characteristics, an increase in pressure results in decreasing drop size and thus in another analogy. Although the vertical distribution of the impinging drop quantity can be controlled by adjusting the nozzle's angle, the decreasing drop size with the spray-off angle can only be realized to a limited extent due to the largely homogeneous spray cone and therefore represents a limitation of the test bench. Another limitation results from neglecting tire design, which is a potential influencing factor, as geometry and tire depth affect the water amount that can remain attached to the tire after lift-off. This factor requires individual investigations, which are beyond the scope of this article. Nevertheless, the realistic simulation of exemplary spray water patterns can be implemented, which enables reproducible investigations. A total of ten different scenarios are simulated at the test bench that exemplarily represent a defined degree of road surface wetness and wheel speed. Table II summarizes the realized scenarios in dependence of the relevant parameters. Here, the class and speed assignments are selected according to the investigations from [6].

For systematic data acquisition at the test bench, each of the ten scenarios defined in Table II is recorded under constant ambient conditions with water of ten representative conductivities summarized in Table III. For each of these conductivities, determined by a conductivity meter [25], the scenarios are recorded with ten measurement series of 90 s. The measurement duration is split into three time segments; the prerun

TABLE II
OVERVIEW OF THE SIMULATED SCENARIOS IN DEPENDENCE ON THE RELEVANT PARAMETERS

Scenario	Class	v [kph]	Nozzle	Angle [°]	Pressure [bar]
S_0	Dry	-	-	-	-
S_{A_1}	Damp	15 ± 5	FCN_a	40	0.7
S_{A_2}		30 ± 10	FCN_a	66	1.5
S_{A_3}		50 ± 10	FCN_a	66	5.0
S_{B_1}	Wet_1	15 ± 5	FCN_b	52	0.5
S_{B_2}		30 ± 10	FCN_b	52	1.5
S_{B_3}		50 ± 10	FCN_b	54	5.0
S_{C_1}	Wet_2	15 ± 5	FCN_c	54	0.5
S_{C_2}		30 ± 10	FCN_c	54	1.5
S_{D_1}	Very wet	15 ± 5	FCN_d	62	0.5
S_{D_2}		30 ± 10	FCN_d	62	1.5

TABLE III
ELECTRICAL CONDUCTIVITY σ-SPECIFIC SAMPLE NUMBERS OF THE DATASET

	σ [µS/cm]	Number of samples
σ_1	2 ± 1	5,850
σ_2	10 ± 1	5,850
σ_3	20 ± 1	5,850
σ_4	30 ± 1	5,850
σ_5	60 ± 1	5,850
σ_6	100 ± 1	5,850
σ_7	396 ± 5	5,850
σ_8	800 ± 5	5,850
σ_9	$2,000 \pm 5$	5,850
σ_{10}	$5,000 \pm 6$	5,850

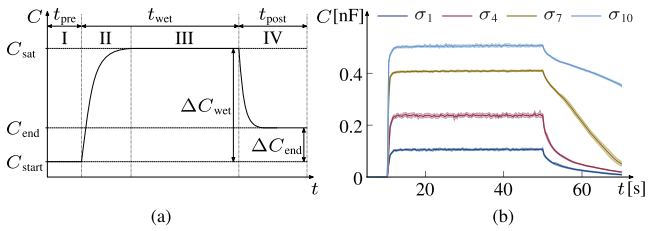

Fig. 3. (a) Schematic representation showing the idealized capacitance characteristic of a TD with impinging spray water. (b) Mean capacitance with standard deviation (shaded) for an exemplary scenario (S_{C_2}) and TD position (P_{22}; see Fig. 1) of four conductivities σ.

segment $t_{pre} = 10$ s, the simulated road surface wetness segment $t_{wet} = 40$ s, and the postrun segment $t_{post} = 40$ s.

Fig. 3(a) shows the schematic representation of the idealized capacitance curve of a TD for one measurement run. Since the relative capacitance change transmitted by the sensor electronics neglects the TD's basic capacitance and due to idealized conditions at the test bench, C_{start} equals zero in the prerun segment (I) that simulates a dry road section. As a result of the impinging water drops, the capacitance increases to a value C_{sat} characteristic of the simulated scenario (II). In region III, the capacitance fluctuates around C_{sat} with a standard deviation due to the stochastic component of the continuously impinging and draining water drops. As no further drops impinge on the TD, the capacitance decreases due to the running-off water in region IV to C_{end} which is defined by the number of remaining drops.

Although the individual scenarios and thus exemplary spray patterns are reproducible, the varying electrical conductivity results in significant differences in the capacitance curves of a scenario. Fig. 3(b) shows the capacitance curves of an example scenario (S_{C_2}) averaged over ten runs for one TD and four conductivities. As the figure indicates, the conductivity-related deviations are high compared to the fluctuation around C_{sat}, thus complicating the distinction of wetness levels.

III. Classification

To evaluate the feasibility of classifying wetness levels in the presence of varying electrical conductivity for the realized scenarios, corresponding investigations are carried out in this section. After describing the fundamental framework for classification, we discuss the results with respect to the conductivity's effect on classifier performance and introduce a two-stage classification approach subsequently.

A. Fundamental Framework

For the classification into wetness levels, the individual measurement series with a length of 90 s is split into segments of 100 sample points, considering the sensor system's sampling rate, and assigned to one of the five classes from Table II. Due to the comparatively large portion of the pre- and postrun time (in total 50 s), representing the class dry, there is an imbalance of the classes that can lead to problems in the classifier evaluation. A frequently used method in literature for balancing the dataset is random undersampling that implements a random elimination of samples belonging to the overrepresented classes [26]. A drawback of this method is that potentially valuable data can be discarded as well as the original distribution is altered [27]. However, since an arbitrary amount as well as reproducible measurement data can be generated at the test bench and furthermore, the original distribution does not contain relevant information, the drawbacks can be considered negligible here. Considering the segments of 100 sample points as well as the random undersampling, the acquired measurement data result in 58 500 samples, where each class of a conductivity σ_i comprises 1170 samples.

Within this article, the accuracy (ACC) is used to evaluate a classifier, which is the most widely applied evaluation metric for balanced datasets and is defined as the ratio of correctly classified samples to the total number of samples [26], [28]. In addition, we use a feature selection algorithm as features can correlate with each other and be counterproductive to the decision process [29]. Besides complexity and training time reduction, a key advantage of feature selection is the potential increase in classifier performance [30], [31]. In this article, we use sequential forward selection (SFS). SFS is a bottom-up search strategy successively adding features selected by an evaluation metric to an empty feature set until no further performance increase can be achieved by additional features. It has the advantage of being robust to overfitting and also has comparatively low computational costs [29], [30].

Furthermore, a k-nearest neighbor (KNN) classifier with Euclidean distance metric is used to classify wetness levels in this article. In order to predict a class, KNN identifies k points in training data with the smallest distance to the test sample to be assigned. In order to determine an optimal k, one reliable way is to perform cross-validation tests with various values and select the highest performing k, which often yields excellent predictive performance [32]. For the present dataset, the highest classifier performance has been achieved for $k = 5$. In addition, KNN has been compared with other conventional learning algorithms, including a decision tree, a support vector machine, and a naive Bayes classifier. For the present dataset, KNN has achieved the highest ACC and is therefore considered for the following investigations.

In this article, we use a total of 272 features comprising 34 features per TD. Table IV summarizes the features used for each TD. Besides common statistical attributes for the whole segment of 100 sample points related to the capacitance vector $\mathbf{C}$ and its time derivative $\mathbf{C}'$, we also implement features covering a fixed number of sample points related to the standard deviation $\mathbf{s}$ of vector $\mathbf{C}$. Here, the index represents the interval size considered.

B. Effect on Classifier Performance

In order to study the effect of electrical conductivity on classifier performance, the underlying dataset $\mathcal{D}$ is partitioned into different training datasets $\mathcal{D}_t$ and validation datasets $\mathcal{D}_v$ for partial investigations. Fig. 4 shows this partitioning for each partial examination (a)–(e).

The first partial investigation (a) is performed for the electrical conductivity σ_7 representing tap water. Here, the associated samples are only considered in the training dataset,

TABLE IV
OVERVIEW OF THE FEATURES USED FOR EACH TD

Index	Feature	Index	Feature
1	Maximum	18	Mean smallest 20 %
2	Minimum	19	Mean $\mathbf{C}'$
3	Median	20	Maximum $\mathbf{C}'$
4	Mean	21	Minimum $\mathbf{C}'$
5	Variance	22	Max. magnitude $\mathbf{C}'$
6	Standard deviation	23	Maximum $\mathbf{s}_{25}$
7	Signal energy	24	Minimum $\mathbf{s}_{25}$
8	Root mean square	25	Mean $\mathbf{s}_{25}$
9	Range	26	Maximum $\frac{\mathbf{s}_{25}}{\overline{\mathbf{C}}_{25}}$
10	Skewness	27	Minimum $\frac{\mathbf{s}_{25}}{\overline{\mathbf{C}}_{25}}$
11	Kurtosis	28	Mean $\frac{\mathbf{s}_{25}}{\overline{\mathbf{C}}_{50}}$
12	Delta	29	Maximum $\mathbf{s}_{50}$
13	Mean largest 5 %	30	Minimum $\mathbf{s}_{50}$
14	Mean largest 10 %	31	Mean $\mathbf{s}_{50}$
15	Mean largest 20 %	32	Maximum $\frac{\mathbf{s}_{50}}{\overline{\mathbf{C}}_{50}}$
16	Mean smallest 5 %	33	Minimum $\frac{\mathbf{s}_{50}}{\overline{\mathbf{C}}_{50}}$
17	Mean smallest 10 %	34	Mean $\frac{\mathbf{s}_{50}}{\overline{\mathbf{C}}_{50}}$

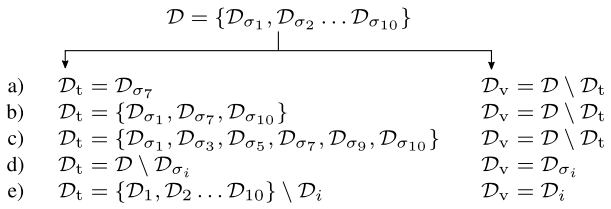

Fig. 4. Partitioning of the dataset $\mathcal{D}$ into training datasets $\mathcal{D}_t$ as well as validation datasets $\mathcal{D}_V$ considering the partial investigation with regard to electrical conductivity.

while the validation of the classifier is performed based on the samples of the other conductivities. Table V shows the mean ACCs obtained from ten runs of the individual conductivities for each partial investigation. The results for subconsideration (a) show that classification of wetness levels with conductivities differing from the training dataset results in a significant performance decrease. While the ACC for a classifier implemented for comparison that considers merely σ_7 in both the training and validation datasets is above 0.99, here it averages about 0.49 over the considered conductivities. In particular, for low conductivities significantly deviating from σ_7, low ACCs of below 0.31 are obtained. The addition of two further subsets to the training dataset (b), which include the lowest as well as the highest conductivity, yields only local improvements and a mean ACC increase of about 0.04. As subconsideration (c) shows that a significant increase in classifier performance can be achieved if the conductivities considered in the training dataset are closer to and enclose those of the validation dataset. In contrast to (b), the distances between the conductivities in the training dataset are small enough to allow interpolation of the unseen conductivities.

Similar results are yielded for subconsideration (d), where the training dataset comprises all conductivities, excluding the currently considered conductivity σ_i. While high ACCs are already achievable in some cases, the subset around conductivity σ_1, in particular, shows drawbacks. For the validation dataset of this conductivity, which results in the lowest absolute capacitances compared to the other conductivities, an ACC of 0.76 is achieved while the others are above 0.87. Considering samples of all conductivities in the training dataset and performing tenfold cross-validation as in subconsideration (e), the mean ACC can be increased to approximately 0.98. Thus, the prerequisite for a high classifier performance is an exhaustive training dataset from a wide range of conductivities.

TABLE V
MEAN ACCS OBTAINED FROM TEN RUNS FOR VARYING PARTITIONS OF THE DATASET $\mathcal{D}$ ACCORDING TO FIG. 4

	σ_1	σ_2	σ_3	σ_4	σ_5	σ_6	σ_7	σ_8	σ_9	σ_{10}	mean
a)	0.29	0.30	0.31	0.28	0.58	0.77		0.68	0.59	0.59	0.49
b)		0.75	0.32	0.22	0.36	0.61		0.57	0.87		0.53
c)		0.95		0.88		0.97		0.96			0.94
d)	0.76	0.96	0.95	0.90	0.99	0.96	0.87	0.93	0.91	0.97	0.92
e)	0.94	0.98	0.97	0.98	0.99	0.99	0.99	0.99	0.98	0.99	0.98

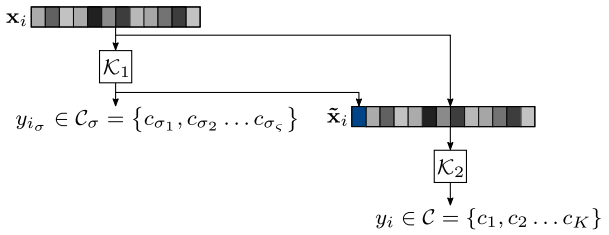

Fig. 5. Two-stage classification approach for considering the spray water's electrical conductivity.

C. Optimization

As shown in the previous section, a classification of wetness levels with varying electrical conductivity is feasible. For this purpose, the conductivity-related differences of the individual capacitance curves are considered by associated samples without information about the actual conductivity. With respect to a potential classifier optimization, the research question is whether the knowledge about the current conductivity can result in an improvement of classifier performance. To this end, corresponding investigations are presented in this section. In this context, the question is also addressed whether the typically unknown electrical conductivity of the impinging spray can be classified using the known features generated from the capacitance curves.

To consider the spray water's electrical conductivity within the classification, a two-stage approach is proposed according to Fig. 5. Classifier $\mathcal{K}_1$ assigns a class $y_{i_\sigma} \in \mathcal{C}_\sigma = \{c_{\sigma_1}, c_{\sigma_2}, \ldots, c_{\sigma_\varsigma}\}$ to a feature vector $\mathbf{x}_i$, where ς represents the number of different conductivities. The predicted conductivity subsequently functions as an additional feature in the modified feature vector $\tilde{\mathbf{x}}_i$, which is assigned to one of K wetness classes by classifier $\mathcal{K}_2$. The two classifiers are implemented analogously to the previous section using a KNN classifier ($k = 5$) with SFS and tenfold cross-validation. To increase statistical confidence, 100 SFSs are performed for each of the classifiers considered. Table VI summarizes the results in the arithmetic mean as well as for the respective SFS showing the highest classifier performance denoted as best.

TABLE VI
CLASSIFIER COMPARISON FOR CONSIDERATION OF ELECTRICAL CONDUCTIVITY

Classifier	ACC		Number of features	
	mean	best	mean	best
$\mathcal{K}_1$	0.9713	0.9729	19.2	19
$\mathcal{K}_{2,\mathrm{opt}}$	0.9959	0.9964	18.6	21
$\mathcal{K}_{2,\mathrm{pred}}$	0.9909	0.9921	18.1	25
$\mathcal{K}_0$	0.9802	0.9831	26.2	30

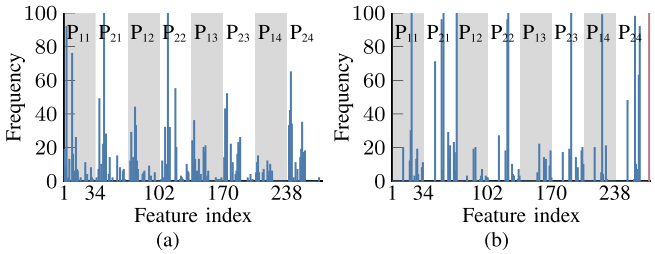

Fig. 6. Selection frequency of each feature during the 100 runs of the SFSs for (a) $\mathcal{K}_1$ and (b) $\mathcal{K}_{2,\mathrm{pred}}$, in dependence on the TD position P_{xz} (see Fig. 1).

Classifier $\mathcal{K}_1$ is developed by assigning zero conductivity to the class dry in the corresponding feature vectors in the training dataset since no spray water is expected and therefore no conductivity can be determined. Thus, a feature significantly correlated with the class dry is already generated in classifier $\mathcal{K}_1$. As the results from Table VI show, the conductivities can be classified from the spray with an ACC of over 0.97 at 19 features selected. In particular, the high classifier performance can be attributed to common statistical features as well as the interaction of different TDs. Fig. 6(a) shows the feature frequency in the 100 runs of SFSs for all 272 features comprising 34 features per TD. We use a continuous feature index for the illustration. The ten most frequently selected features comprise exclusively common classical features with regard to $\mathbf{C}$, which are represented by TD-related low indices (see Table IV), since, in particular, the absolute capacitance contains essential information for conductivity classification. As the amount of impinging spray water, with which the absolute capacitance is correlated, is unknown, the different TD positions are also relevant and therefore all considered within the SFSs. A classification of the spray water's electrical conductivity is thus feasible and enables potential in further application areas beyond the realization of the two-stage approach for the quantification of wetness levels.

In order to evaluate the performance gain by knowledge of the current electrical conductivity, the classifier $\mathcal{K}_{2,\mathrm{opt}}$ is developed assuming an optimally classifying $\mathcal{K}_1$ and compared with the single-stage classifier $\mathcal{K}_0$. As shown in Table VI, the ACC can be increased by over 0.01–0.996. Also, the classifier $\mathcal{K}_{2,\mathrm{pred}}$, using the conductivities assigned by $\mathcal{K}_1$ as a feature, can significantly increase classifier performance compared to $\mathcal{K}_0$. Accordingly, knowledge of the spray's present conductivity enables an optimized prediction of the wetness level. Fig. 6(b) indicates the feature's significance, too. The conductivity (represented by the last bar) is selected in each of the 100 SFSs for $\mathcal{K}_{2,\mathrm{pred}}$. In addition, features related to the capacitance change as well as the standard deviation are selected more frequently, whereas the selection of classical features, as for classifier $\mathcal{K}_1$, is rare. All in all, the two-stage classifier is shown to significantly increase the performance.

IV. CONCLUSION

In this article, we studied the effect of the spray water's electrical conductivity on road surface wetness classification. To this end, we generated reproducible spray water scenarios representing a specific wheel speed and a road surface wetness class. For data acquisition by a capacitive sensor system, the scenarios were simulated with ten different water conductivities. Measurement results for an exemplary spray water scenario have demonstrated the effect of varying conductivity on the capacitance curves motivating the subsequent investigations with respect to classifier performance.

Conductivity-specific partitioning of dataset $\mathcal{D}$ provided various partial investigations that demonstrated the extent of the conductivity's effect on classifier performance. We have shown that excluding the different conductivities from the training dataset $\mathcal{D}_t$ results in a weak mean performance of 0.49 for the validation dataset $\mathcal{D}_v$ containing various conductivities. In particular, conductivity data that differ significantly from those considered in the training dataset contribute to low performance. A significant mean performance increase to 0.94 can be achieved if the conductivities considered in $\mathcal{D}_t$ enclose those of $\mathcal{D}_v$, allowing an interpolation of the unknown conductivities. In addition, consideration of all occurring conductivities in the training dataset can increase the mean performance to 0.98. Thus, an extensive database containing a wide range of conductivity variations is essential for a reliable road surface wetness classification based on capacitive measurement data.

Furthermore, we have shown that knowledge of the spray's present conductivity results in a significant performance increase to above 0.99. For optimization, we introduced a two-stage classification approach that initially determines the conductivity and subsequently considers it as an additional feature in the classification of the present wetness level. In this context, we have also demonstrated that a classification of the spray water's electrical conductivity using capacitive measurement data is feasible.

Future work will include investigations on test tracks and public roads to validate the transferability of the results presented in this article.

REFERENCES

[1] C. Ahn, H. Peng, and H. E. Tseng, "Robust estimation of road frictional coefficient," *IEEE Trans. Control Syst. Technol.*, vol. 21, no. 1, pp. 1–13, Jan. 2013.

[2] C.-G. Wallman and H. Aström, *Friction Measurement Methods Correlation Between Road Friction Traffic Safety. A Literature Review*. Linköping, Sweden: Swedish National Road and Transport Research Institute (VTI), 2001.

[3] H. Brodsky and A. Hakkert, "Risk of a road accident in rainy weather," *Accident Anal. Prevention*, vol. 20, no. 3, pp. 161–176, 1988.

[4] A. G. Kokkalis and O. K. Panagouli, "Fractal evaluation of pavement skid resistance variations. I: Surface wetting," *Chaos, Solitons Fractals*, vol. 9, no. 11, pp. 1875–1890, Nov. 1998.

[5] R. Lamm, E. M. Choueiri, and T. Mailaender, "Comparison of operating speeds on dry and wet pavements of two-lane rural highways," *Transp. Res. Rec.*, vol. 1280, no. 8, pp. 199–207, 1990.
[6] J. Döring, A. Beering, J. Scholtyssek, and K.-L. Krieger, "Road surface wetness quantification using a capacitive sensor system," *IEEE Access*, vol. 9, pp. 145498–145512, 2021.
[7] G. G. Raju, *Dielectrics in Electric Fields: Tables, Atoms, and Molecules*. Boca Raton, FL, USA: CRC Press, 2017.
[8] K. C. Kao, *Dielectric Phenomena in Solids*. Amsterdam, The Netherlands: Elsevier, 2004.
[9] S. M. Huang, R. G. Green, A. B. Plaskowski, and M. S. Beck, "Conductivity effects on capacitance measurements of two-component fluids using the charge transfer method," *J. Phys. E, Sci. Instrum.*, vol. 21, no. 6, pp. 539–548, 1988.
[10] G. Behzadi and H. Golnabi, "Comparison of invasive and non-invasive cylindrical capacitive sensors for electrical measurements of different water solutions and mixtures," *Sens. Actuators A, Phys.*, vol. 167, no. 2, pp. 359–366, 2011.
[11] Q. Yang *et al.*, "An inkjet-printed capacitive sensor for water level or quality monitoring: Investigated theoretically and experimentally," *J. Mater. Chem. A*, vol. 5, no. 34, pp. 17841–17847, 2017.
[12] J. Happel, J. Doering, and K.-L. Krieger, "Capacitive sensors for contactless level and composition measurement in automotive clear vision systems," in *Proc. Sensors Measuring Syst., 19th ITG/GMA-Symp.*, Jun. 2018, pp. 1–4.
[13] M. Zdeb, D. Papciak, and J. Zamorska, "An assessment of the quality and use of rainwater as the basis for sustainable water management in suburban areas," in *Proc. E S Web Conf.*, vol. 45, Jul. 2018, pp. 1–8.
[14] M. I. Yaziz, H. Gunting, N. Sapari, and A. W. Ghazali, "Variations in rainwater quality from roof catchments," *Water Res.*, vol. 23, no. 6, pp. 761–765, Jun. 1989.
[15] U. Tegethof, *Straßenseitige Belastungen des Grundwassers* (Berichte der Bundesanstalt für Straßenwesen), vol. 60, V. Verkehrstechnik and V. Heft, Eds. Bremerhaven, Germany: Wirtschaftsverlag NW, 1998. [Online]. Available: https://trid.trb.org/view/962680
[16] E. Makineci, M. Demir, and M. Kartaloglu, "Acidity (pH) and electrical conductivity changes in runoff water from ditches of paved and unpaved forest roads," *Baltic Forestry*, vol. 21, no. 1, pp. 170–175, Jan. 2015.
[17] E. Skarbøvik and R. Roseth, "Use of sensor data for turbidity, pH and conductivity as an alternative to conventional water quality monitoring in four Norwegian case studies," *Acta Agriculturae Scandinavica, B, Soil Plant Sci.*, vol. 65, no. 1, pp. 63–73, Jan. 2015.
[18] J. Döring, D. Lepke, and K.-L. Krieger, "Design of planar capacitive transducers for the detection of road surface wetness," in *Sensor and Measurement Science International*. Wunstdorf, Germany: AMA Service GmbH, 2020, pp. 250–251.
[19] *FDC2112-Q1, FDC2114-Q1, FDC2212-Q1, FDC2214-Q1 Multi-Channel 12-Bit or 28-Bit Capacitance-to-Digital Converter (FDC) for Capacitive Sensing*, Texas Instruments, Dallas, TX, USA, 2016.
[20] B. Schmiedel, F. Gauterin, and H.-J. Unrau, "Study of system layouts for road wetness quantification via tire spray," *Automot. Engine Technol.*, vol. 4, nos. 1–2, pp. 63–73, 2019.
[21] I. Spruß, "Ein beitrag zur untersuchung der kraftfahrzeugverschmutzung in experiment und simulation," Ph.D. dissertation, Universität Stuttgart, Stuttgart, Germany, 2016.
[22] *Vollkegeldüe DBL*, DIVA Sprühtechnik GmbH, Hamburg, Germany, 2019.
[23] *Vollkegel-Düsen VGB*, MC GmbH, Ostfildern, Germany, 2019.
[24] *Vollkegeldüse DBIM/DBIF*, DIVA Sprühtechnik GmbH, Hamburg, Germany, 2019.
[25] *Operating Manual Conductivity Measuring Instrument GLF 100*, GHM Messtechnik GmbH, Regenstauf, Germany, 2010.
[26] Y. Sun, A. K. Wong, and M. S. Kamel, "Classification of imbalanced data: A review," *Int. J. Pattern Recognit. Artif. Intell.*, vol. 23, no. 4, pp. 687–719, 2009.
[27] S. Kotsiantis, D. Kanellopoulos, and P. Pintelas, "Handling imbalanced datasets: A review," *GESTS Int. Trans. Comput. Sci. Eng.*, vol. 30, no. 1, pp. 25–36, 2006.
[28] G. M. Weiss, "Mining with rarity: A unifying framework," *ACM SIGKDD Explorations Newslett.*, vol. 6, no. 1, pp. 7–19, Jun. 2004.
[29] V. Kotu and B. Deshpande, *Data Science: Concepts Practice*. Burlington, MA, USA: Morgan Kaufmann, 2018.
[30] I. Guyon and A. Elisseeff, "An introduction to variable and feature selection," *J. Mach. Learn. Res.*, vol. 3, pp. 1157–1182, May 2003. [Online]. Available: http://dl.acm.org/citation.cfm?id=944919.944968
[31] D. Mladenic, "Feature selection for dimensionality reduction," in *Statistical and Optimization Perspectives Workshop*. Berlin, Germany: Springer, 2005, pp. 84–102.
[32] I. H. Witten, C. J. Pal, E. Frank, and M. A. Hall, *Data Mining: Practical Machine Learning Tools Techniques*, 4th ed. Cambridge, MA, USA: Morgan Kaufmann, 2017.

Jakob Döring received the B.Sc. and M.Sc. degrees in electrical and information engineering from the University of Bremen, Bremen, Germany, in 2014 and 2017, respectively. He is currently pursuing the Ph.D. degree with the Institute of Electrodynamics and Microelectronics, University of Bremen.

His research interests include capacitive sensors and the classification of road surface wetness.

Lukas Lütkehaus received the B.Sc. degree in systems engineering from the University of Bremen, Bremen, Germany, in 2020. He is currently pursuing the M.Sc. degree with the University of Bremen.

His research interests include automation and robotics and machine learning.

Karl-Ludwig Krieger received the Ph.D. degree in electrical engineering from the University of Bremen, Bremen, Germany, in 1999.

From 1998 to 2009, Dr. Krieger worked as the Manager of Function and Algorithm Development for Powertrain Systems with Daimler AG, Stuttgart, Germany. Since 2009, he has been a Full Professor of the Chair of Electronic Vehicle and Mobility Systems, University of Bremen.